Journal of Structural Geology, Vol. 15, No. 11, pp. 1331 to 1342, 1993
Printed in Great Britain

0191-8141/93 $06.00+0.00

Restoration of cross-sections through unfaulted, variably strained strata

J. H. HOWARD

EST/Earth Science Technologies, P.O. Box 358, Barker, TX 77413, U.S.A.

(*Received* 10 *March* 1992; *accepted in revised form* 22 *October* 1992)

Abstract—Data on the dip of bedding and the state of strain at specific locations within a cross-section constrain the restoration of unfaulted, two-dimensional, variably strained strata. There are two major categories for restoration of such strata. The first is one-step restoration, which involves retro-deforming the strain ellipses into their corresponding unit circles while simultaneously removing dips from associated beds. This procedure is appropriate if strain indicators record the transformation of the strata from the undeformed state to present deformation. The second category pertains to situations in which strain indicators record the transformation of the present deformed state from an intermediate, deformed state. The second category requires multiple step restoration.

For the one-step restoration procedure presented in this paper, the first task is to determine the transformation constants that describe development of observed strain and bedding for each location. The next task is to determine the retro-deformation constants which relate points in their present deformed state to their locations in the undeformed state. Retro-deformation constants are related to the spatial derivatives of the Cartesian retro-deformation displacements functions, $U^*(x,y)$ and $V^*(x,y)$ (for movements in the x and y directions, respectively). The spatial derivatives of these functions at locations of observed strain and the displacements of selected points about these sites are the basis for constructing continuous, retro-deformation displacements functions for the deformed section as a whole. The retro-deformation displacements functions are then invoked to restore the cross-section.

This procedure is illustrated with an example cross-section from the Appalachian Fold Belt, and the example shows that the section may be satisfactorily restored in this way.

It is just as likely, however, that the strain indicators for the example section are a measure of the transformation of the cross-section from a prior, deformed state to the present deformation. Accordingly, multiple-step restoration is required, first to an intermediate, less deformed state and then to the undeformed state. Two sets of retro-deformation displacement functions are then needed, i.e. one set for transformation to an intermediate state followed by a second to the undeformed state. This procedure was done for the Appalachian fold–thrust belt example, restoring first the present deformed section to an intermediate state derived from the regional fold history. In turn, intermediate state points were transformed to an undeformed state assuming knowledge of an undeformed stratal thickness and assuming that cross-sectional area has been preserved. This procedure is technically different to that used in the one-step procedure, but conceptually similar. The objective, once again, is to discover appropriate retro-deformation displacements functions.

INTRODUCTION

THIS paper describes one-step and multi-step procedures for restoration of unfaulted, variably-strained cross-sections. The one-step procedure is described first and is appropriate if strain indicators record the transformation of the strata from the undeformed state to present deformation. The second procedure requires multiple-step restoration and pertains to situations in which strain indicators record the transformation of the present deformed state from an intermediate, deformed state. An example cross-section from the Appalachian fold–thrust belt illustrates both procedures. The example shows that the section may be satisfactorily restored with either procedure. However, the interpretation assigned to the strain indicators differs. For the one-step procedure, observed strains are interpreted as a measure of transformation from an undeformed state. For the multi-step procedure, they record transformation from an intermediate state of deformation.

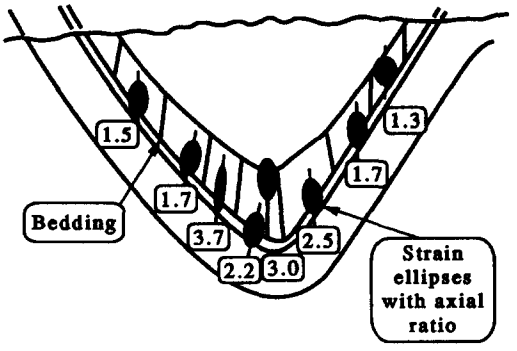

Fig. 1. Sample geologic cross-section. No vertical exaggeration. The strain ellipses provide information at various locations within the cross-section on ratios of principal strains and their orientation in present deformation. Note dip of bedding. After fig. 2(a) of Woodward *et al.* (1986), based on prior work by Reks & Gray (1983).

GIVEN INFORMATION AND ASSUMPTIONS

We are given a deformed geologic cross-section, without vertical exaggeration, within a scaled Cartesian system (Fig. 1). Relative values of strain at points within the cross section are shown graphically by a set of strain ellipses posted at points on the section (Fig. 1).

We assume that strains are homogeneous about a point and that they vary smoothly from point to point. We also assume that prior to any deformation all bedding planes were horizontal and continuous.

SOLUTION FOR LOCAL RESTORATION OF STRAINS AND BEDDING

Assuming that observed strains record the transformation of the section from an undeformed state to the present deformation, the procedure begins with restoration of strains and bedding locally, i.e. at points of observed strain and their vicinity within the cross-section. The subsequent task involves integration of local restorations in order to restore the cross-section as a whole.

Definitions and symbols

Table 1 lists definitions and symbols involved in the analysis. Figure 2 illustrates the meaning of these definitions.

The transformation constants of finite homogeneous strain, a,b,c and d are fundamental to the analysis. They relate the Cartesian co-ordinates of a point in its undeformed state (x,y) to its position in the present deformation (x', y'):

$$x' = ax + by \quad (1)$$

$$y' = cx + dy. \quad (2)$$

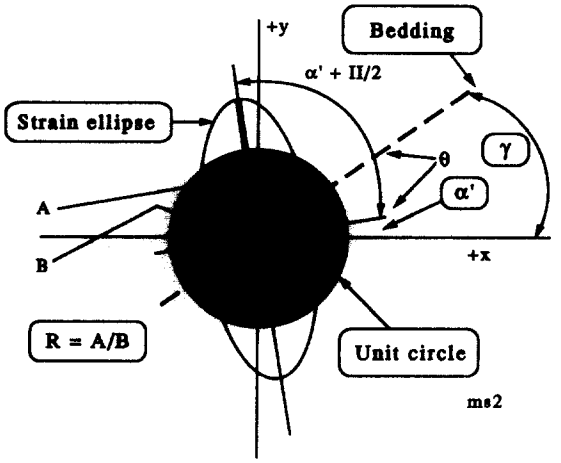

Fig. 2. Key definitions and their symbols. The unit circle is transformed into a strain ellipse describing the present deformation. Bedding, which was originally horizontal, now lies at and angle γ to the $+x$ axis.

Overview of the solution

The solution to the first part of this procedure, which we refer to as '*local* analysis', consists of a series of tasks. The first is determination of the size of the strain ellipse in terms of units of radii of the unit circle. The second is determination of values for two of the transformation constants for deformation by comparing the intersection of bedding and the strain ellipse in present deformation with the intersection of bedding and the unit circle before any deformation, i.e. when bedding was flat. The third task is determination of the remaining two transformation constants for deformation (a) from information on the relative size of the strain ellipse vs the unit circle from which it was transformed and (b) from the orientation of the strain ellipse itself. The next task is determination of values for those transformation constants that will *restore* deformed points to their undeformed positions; these are the *retro-deformation transformation constants*. Next is determination of the spatial gradients of the retro-deformation displacements functions appropriate to the vicinity of the point; they depend on the retro-deformation transformation constants. The final step regarding local restoration is construction of retro-deformation displacements functions locally.

Relative size of the strain ellipse

The areal size of the strain ellipse relative to the unit circle from which it was transformed provides key information for determining the transformation constants involved in the restoration. There are a number of possibilities for relating size of the unit circle to size of its corresponding strain ellipse. However, we will make the very simple assumption that the area of unit circle equals the area of the strain ellipse, i.e. $\pi r^2 = \pi AB$. Then, in order to obtain values for the lengths of the axes of the ellipse in terms of radii of the unit circle:

$$A = \sqrt{(R)} \quad (3)$$

$$B = \sqrt{(1/R)}. \quad (4)$$

Assuming that the area of the ellipse is equal to the area of the unit circle from which it has been transformed, the polar radius in the direction θ of the strain

Table 1. List of symbols and their definitions

Symbol	Definition	Comment
$\alpha', \alpha' + \pi/2$	Orientation of a semi-axis of a particular strain ellipse	Measured counter-clockwise from the $+x$ axis
A,B	Major and minor semi-axes of a strain ellipse, respectively	
R	Ratio of the major to minor axes of the strain ellipse	$R \geq 1$
γ	Angle of bedding in cross-section at point of strain ellipse	Angles reckoned from the $+x$ axis. Angles measured clockwise are negative
θ	Angle between radius of ellipse and a semi-axis of the ellipse	
ρ_θ	Length of a radius of the strain ellipse at angle θ.	
a,b,c,d	Transformation constants of finite homogeneous strain	See equations (1) and (2)
a^*,b^*,c^*,d^*	Retro-deformation transformation constants of strain	See equations (17) and (20)
x,y	Cartesian co-ordinates of a point in its *undeformed condition*	See equations (1) and (2)
x',y'	Cartesian co-ordinates of a point in *present deformation*	See equations (17) and (20)

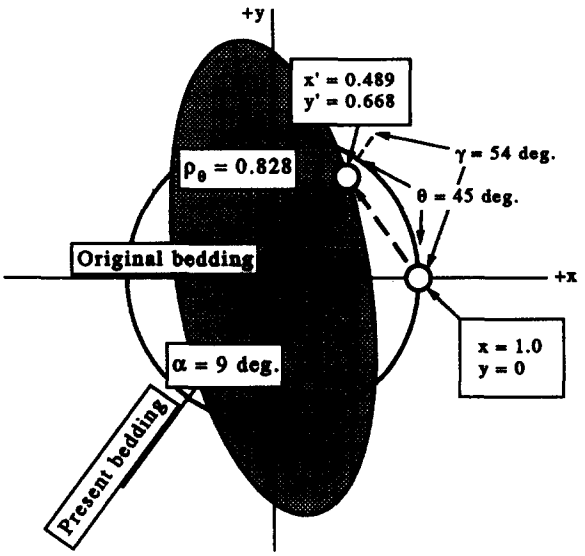

Fig. 3. Illustrative specific example (element 6). Example shows the transformation of a point at the intersection of bedding and the unit circle to the point of intersection of bedding and the strain ellipse in the present deformation.

ellipse with semi-axes A and B, respectively, is given by (e.g. Hodgman 1959):

$$\rho_\theta^2 = \frac{(A^2B^2)}{(A^2\sin^2\theta + B^2\cos^2\theta)}. \tag{5}$$

ρ_θ is always positive.

In the present deformation, the co-ordinates of a point on the strain ellipse at angle θ in Cartesian co-ordinates with origin at the center of the ellipse are x', y' (see Fig. 3). In terms of γ, the angle between the $+x$ axis and a radius of the ellipse which lies at angle θ to a semi-axis, the values x' and y' are given by (Fig. 3):

$$x' = \cos\gamma\,\rho_\theta \tag{6}$$

$$y' = \sin\gamma\,\rho_\theta. \tag{7}$$

For the specific example in Fig. 3, a semi-axis of the strain ellipse makes an angle, α', of 9° with the $+x$ axis and the angle θ between a semi-axis and a line representing present-day bedding is 45°. The angle γ, therefore, is 54°. For this specific example, according to equations (3) and (4), $A = 1.581$ and $B = 0.632$, respectively. The length, ρ_θ, of the radius of the ellipse in this direction in terms of unit circle radii is, according to equation (5), 0.828. The co-ordinates of the intersection of bedding with the strain ellipse are thus from equations (6) and (7), $x' = 0.489$ and $y' = 0.668$ unit circle radii. We use this information to obtain values for two of the transformation constants, a and c.

Determination of a *and* c *from intersection of bedding and strain ellipse*

As a consequence of the movement of points to the present deformation from their prior positions, a point originally at the intersection of bedding and the unit circle must have moved to a new location, namely at the intersection of bedding and the strain ellipse. Furthermore, for this particular point, in terms of unit circle radii, $x = 1$ and $y = 0$.

Hence, from equations (1) and (2),

$$a(1) = x' \tag{1'}$$

$$c(1) = y' \tag{2'}$$

with co-ordinates given in terms of unit circle radii. For the specific example shown in Fig. 3, the transformation constants are $a = 0.489$, $c = 0.668$.

Determination of b *and* d *from the relative size of the strain ellipse and its orientation*

The remaining two transformation constants, b and d, are obtained from information on the relative size of the strain ellipse vs the unit circle from which it was transformed and from the orientation of the strain ellipse itself. Two equations and two unknowns are involved (Jaeger 1956, pp. 25 and 28):

$$AB = ad - bc \tag{8}$$

$$\tan 2\alpha' = \frac{2(ac + bd)}{(a^2 + b^2 - c^2 - d^2)}. \tag{9}$$

Equations (1') and (2') can be combined with equations (8) and (9) to yield an expression for the transformation constant b in quadratic form.

$$b = \frac{(-K_b \pm (K_b^2 - 4K_aK_c)^{1/2})}{(2K_a)}. \tag{10}$$

The angle α' is known. Let $T = \tan 2\alpha'$, then

$$K_b = -\frac{2TABc}{a^2} - \frac{2AB}{a} \tag{11}$$

$$K_a = T - \frac{Tc^2}{a^2} - \frac{2c}{a} \tag{12}$$

$$K_c = Ta^2 - Tc^2 - \frac{TA^2B^2}{a^2} - 2ac. \tag{13}$$

Inasmuch as b is now known, the transformation constant d can be determined from (8):

$$d = \frac{AB}{a} + \frac{bc}{a}. \tag{8'}$$

In fact, there are two sets of values for b and for d, owing to the choice of signs in equation (10). The practical solution for identifying correct values is to determine the location of the point 0,1 unit-radii of the unit circle. The correct choice for transformation constants will move this point onto the strain ellipse in the present deformation.

Cross checks on values for the transformation constants

Several cross checks can be used to confirm that the transformation constants have been correctly determined. First, the value $(ad - bc)$ should equal the product of the semi-axes, AB (Jaeger 1956, pp. 25 and

28). For the special case in which the area of the strain ellipse is equal to the area of the unit circle, $ad - bc$ equals 1. Second, the radii of the unit circle that are transformed into the principal axes of the strain ellipse in the present deformation should now extend at angles, α' and $\alpha' + \pi/2$. The latter cross check requires determination of the angle, α, the angle made by these radii of the unit circle *prior* to present deformation. The angles α (and $\alpha - \pi/2$) also are functions of the transformation constants (Jaeger 1956, p. 26):

$$\tan 2\alpha = \frac{2(ab + cd)}{(a^2 + c^2 - b^2 - d^2)}. \quad (14)$$

Having found α (and therefore $\alpha + \pi/2$), it is necessary to determine the point of intersection of these radii with the unit circle and obtain values for their Cartesian co-ordinates. In turn, these co-ordinates are transformed to the present deformation. The radii of the ellipse passing through these transformed points should lie at angles α' and $\alpha' + \pi/2$.

Determination of the retro-deformation constants

A set of transformation constants exists that will restore the deformed points to their original positions. They are here referred to as the retro-deformation transformation constants and denoted a^*, b^*, c^* and d^*. Equations (1) and (2) involve the transformation constants, a, b, c, and d, which are now known. These equations may be combined and rearranged to yield an expression for the Cartesian co-ordinates of a point prior to present deformation, namely (x,y). Now, however, co-ordinates *prior to present deformation* will be given as a function of co-ordinates in the present deformation (x',y') and a set of *retro-deformation* transformation constants. With $h^2 = ad - bc$, algebraic rearrangement yields:

$$x = \frac{dx'}{h^2} - \frac{by'}{h^2} \quad (15)$$

$$y = \frac{-cx'}{h^2} - \frac{ay'}{-h^2}. \quad (16)$$

Hence, by analogy with equations (1) and (2),

$$a^* = d/h^2 \quad (17)$$

$$b^* = -b/h^2 \quad (18)$$

$$c^* = -c/h^2 \quad (19)$$

$$d^* = a/h^2. \quad (20)$$

If $h^2 = 1$, then $a^* = d$, $b^* = -b$, $c^* = -c$ and $d^* = a$.

Relationship of transformation constants to displacement functions

The difference in position of a point within a fixed reference frame in a prior reference state (x,y) and in its present state (x',y') is its total displacement. For the transformation of a point from its present deformed state to a prior state, the components of total displacement in the x and y Cartesian co-ordinate directions are u^* and v^*, respectively:

$$u^* = x' = x \quad (21)$$

$$v^* = y' - y. \quad (22)$$

The functions that describe the displacements of *all* points in a body transformed from present deformation to a prior state are $U^*(x,y)$ and $V^*(x,y)$ for displacements in the x and y directions, respectively. These may be referred to as the 'global' displacements functions. It can be shown, furthermore, that the following relationships exist between the retro-deformation constants and the derivatives of the displacements functions associated with retro-deformation (Howard 1968a):

$$a^* = 1 + \delta U^*(x,y)/\delta x \quad (23)$$

$$b^* = \delta U^*(x,y)/\delta y \quad (24)$$

$$c^* = \delta V^*(x,y)/\delta x \quad (25)$$

$$d^* = 1 + \delta V^*(x,y)/\delta y. \quad (26)$$

Thus, if a^*, etc, are known at a point, we can compute values for $\delta U^*/\delta x$, etc., appropriate to the points where values of a^*, etc., apply.

Summary

We summarize our analysis of this procedure to this point as follows. If we know the state of strain and the attitude of bedding locally in present deformation, we can restore to an undeformed, flat-bedded state. We can determine the transformation constants a, b, c and d, and, then, the retro-deformation constants, a^*, b^*, c^* and d^*. Furthermore, owing to the relationships in equations (23)–(26), we can locally constrain the form of the retro-deformation displacements functions, $U^*(x,y)$ and $V^*(x,y)$. These functions must yield local derivatives consistent with calculations from equations (23)–(26).

RETRO-DEFORMATION AND ASSEMBLY OF INDIVIDUAL ELEMENTS

Pertinent information

Figure 1 (taken from fig. 2a in Woodward *et al.* 1986) will be used to illustrate *local* restoration. By 'local restoration' we mean restoration of each of the elements shown on Fig. 1. Figure 4 shows these elements more clearly, and they have been numbered 1–8. Table 2 lists key parameters associated with each of these elements. Figure 4 is based on fig. 5 in Woodward *et al.* (1986). Table 2 also lists co-ordinates for the corner points of these elements. Corner points are listed clockwise beginning at upper left-hand corner point of each element. They are reported with respect to a conveniently chosen origin as shown in the lower left-hand side of Fig. 4(a).

Restoration and assembly of individual elements of the cross-section

Local values for the derivatives of the retro-deformation displacements functions are key to the restoration of the cross-section as a whole. In this section, we present a method of restoration similar to Woodward *et al.* (1986, their fig. 5b). However, in our restoration, bedding at the bottom of the elements is required to be flat and continuous. For each element, we set up a local co-ordinate system with origin placed midway along the base of the element. We assume, for now (see below), that the displacements functions are planar over the extent of each element, i.e. that the spatial gradients of the functions are constant and that strain is homogeneous within each element. We integrate the derivatives $\delta U^*(x,y)/\delta x$, etc., and set the constant of integration equal to zero. Thus, we can determine the displacements of the corner points of each element by setting the increments, δx, etc., from local origins to all corners equal to the x and y distances from the origin to each corner. This procedure defines an approximate shape for the element prior to deformation. We may subsequently join each of the restored elements along their bases to yield the cross-section shown in Fig. 6. This restoration may be compared with Fig. 5 (Woodward *et al.* 1986, their fig. 5a). Obviously, there are mismatches of adjacent restored elements because mismatches between neighboring elements were not taken into account except along their bases. Mismatches can be eliminated by constructing *continuous* functions as explained in the following section.

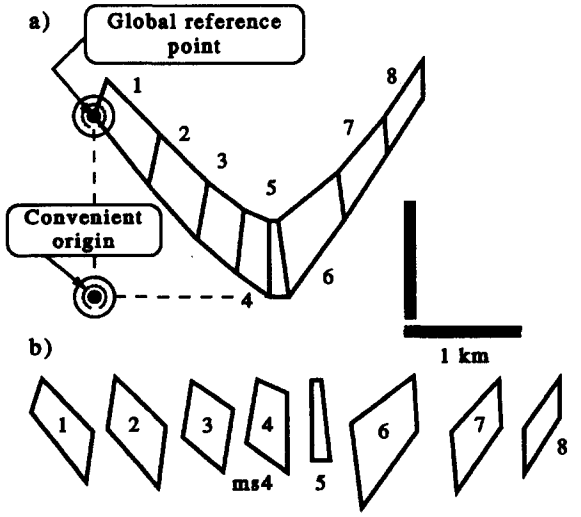

Fig. 4. Elements of the sample cross-section. (a) Elements, idealized and simplified, of a deformed example cross-section with scale. The positions of the corners of the eight elements that make up the cross-section can be stated in terms of a convenient origin (lower left). (b) An exploded view of the individual elements.

CONSTRUCTION OF CONTINUOUS FUNCTIONS AND RESTORATION OF WHOLE CROSS-SECTIONS

Integrating elements to yield continuous functions

Our procedure in this paper for constructing *continuous* functions involves two main sets of calculations. The first concerns calculation of values of displacement for the bases of all elements with respect to a single, fixed point within the cross-section. The second concerns calculation of the trend of constant values for the retro-deformation displacements functions midway along the base of each element for all the elements. The first calculation determines the magnitudes of the displacement of selected points of the cross-section relative to a single fixed point. The second calculation provides information about the trend of lines of equal magnitude of $U^*(x,y)$ and of $V^*(x,y)$. In other words, the second calculation determines the orientation of *iso-displacement lines*. Together, this information provides the basis for interpolating continuous functions. In geologic terms, our problem is analogous to using elevation and strike and dip readings at separate points on a continuous surface to construct a structure contour map of the surface. Here, however, we wish to determine 'contour maps' of the functions $U^*(x,y)$ and $V^*(x,y)$. Such maps will allow us to read specific values of u^* and v^* at all points within the cross-section and thus bring about a restoration.

In order to carry out these calculations, we define an indexing system for tracking points. The indexing system uses a pair of numbers (i.e. M,N) to identify points on the cross-section. This pair is used to tag various items of information including values for the functions U^* and V^* at selected points of the cross-section. The first number refers to the element; the second number

Table 2. List of values for certain key parameters for elements of the cross-section. Included are element number, R, γ, α', θ and co-ordinates of corner points of each element with respect to the convenient origin shown in Fig. 4

Element No.	R	γ	α'	θ	$X1^*$	$Y1$	$X2$	$Y2$	$X3$	$Y3$	$X4$	$Y4$
1	1.5	−52.43145226	−6	−46.4315	0.1	2.05	0.58	1.54	0.50	1.07	0.00	1.72
2	1.7	−48.57637541	−14	−34.5764	0.58	1.54	1.05	1.09	0.95	0.56	0.5	1.07
3	3.7	−42.43626563	−5	−37.4363	1.05	1.09	1.39	0.84	1.3	0.24	0.95	0.56
4	2.2	−35.21762272	−16	−19.2176	1.39	0.84	1.64	0.72	1.64	0	1.3	0.24
5	3	0	3	−3	1.64	0.72	1.71	0.73	1.8	0	1.64	0
6	2.5	53.78120816	9	44.78121	1.71	0.73	2.27	1.18	2.32	0.71	1.8	0
7	1.7	56.30998004	3	53.30998	2.27	1.18	2.72	1.7	2.74	1.34	2.32	0.71
8	1.3	59.48981284	4	55.48981	2.72	1.7	3.07	2.22	3.07	1.9	2.74	1.34

*Measured in km; with respect to convenient origin.

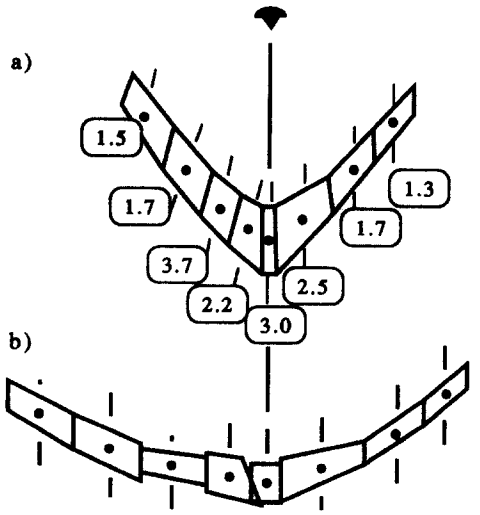

Fig. 5. Simplified version of Fig. 1. (a) Elements of the cross-section in the present deformation as proposed by Woodward *et al.* (1986), based on prior work by Reks & Gray (1983). Numbers refer to values for the ratio of major/minor radii of the ellipse; cf. Figs. 1 and 4. (b) Restoration proposed by Woodward *et al.* (1986), based on prior work by Reks & Gray (1983).

refers to a particular corner point of the element. The corners are *numbered clockwise* with the first point (1) taken at the upper left of a quadrilateral element. For example, $x(M,N)$ refers to the location within a reference frame of the Nth point in the Mth element. $u^*(M,N)$ refers to the retro-deformation displacement in the x direction of the Nth point in the Mth element.

From calculations explained above, we know the displacements required for retro-deformation of the corners of each element with respect to a local origin set midway along the base of each element. We specify the lower left-hand corner of element 1 as the fixed point from which all displacements of all elements will be reckoned. This point is the global reference point on Fig. 4. In terms of the indexing scheme, this point is (1,4) (i.e. first element, fourth point of the quadrilateral).

The origin of each of the elements is:

$$x = \frac{x(M,3) - x(M,4)}{2} \tag{27}$$

$$y = \frac{y(M,4) - y(M,3)}{2}. \tag{28}$$

Our procedure for adjusting displacements to the global reference point involves repetitious shifts of local origins and corner points *along the base of an element* for each element. We assure continuity among elements by requiring continuity along the base of the elements and by drawing the functions elsewhere guided by values along the baseline and by iso-displacements line (see below).

In order to restore element 1 with respect to the local origin, the point 1,4 was to be displaced an amount $u^*(1,4)$. However, if point (1,4) is to remain fixed, we must now add a displacement $[-u^*(1,4)]$, to it. The result is zero, which is appropriate because we wish the point (1,4) to be a fixed global reference point from which all other displacements are reckoned. Likewise, we must add $[-u^*(1,4)]$ to the displacement of the origin. Its displacement in the x direction had been zero as a consequence of the manner of integrating the derivatives of $U^*(x,y)$. Now, with respect to the global reference point, this displacement becomes $0 + [-u^*(1,4)]$. Similarly, the value for displacement in the x direction of the point (1,3) had been $u^*(1,3)$. With respect to the global reference point, this displacement becomes $u^*(1,3) + u^*(1,4)$.

The same procedure is applied in order to determine values of displacement in the y direction. With respect to the global reference point, $v^*(1,4)$ becomes zero. The displacement of the origin is adjusted to $[-v^*(1,4)]$. $v^*(1,3)$ is adjusted to $v^*(1,3) + v^*(1,4)$.

A complication arises as adjacent elements are joined. Point 3 of the first element (1,3) and point 4 of the second element (2,4) are the same point. Consequently, when displacements for the *second* element are shifted to give displacements relative to the fixed point, they must be done with respect to point $(M,3)$ of the prior element. For example, the displacement of point (2,4) in the x direction, namely $u^*(2,4)$, must equal $u^*(1,3)$. Displacement in the x direction of the local origin of the second element must take into account displacement with respect to the point (2,4) within the framework of

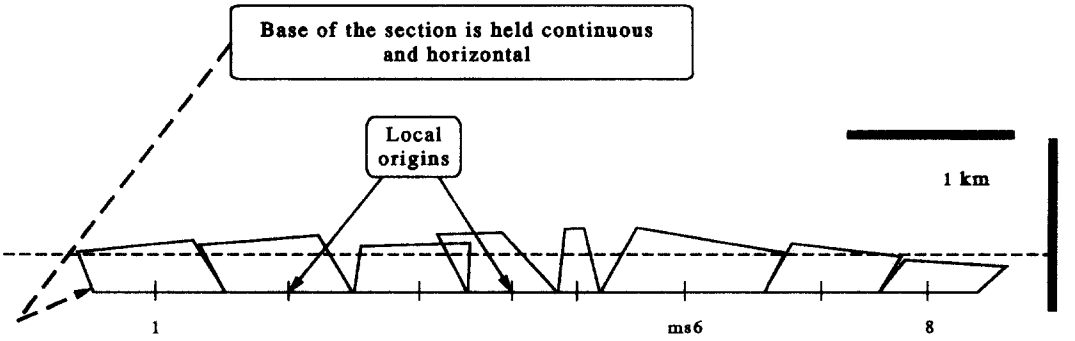

Fig. 6. Piecemeal restoration of the cross-section shown in Fig. 1 using restored versions of the elements shown in Fig. 4. The base of each element has been flattened and joined graphically with bases of adjacent elements to produce a flat, continuous basal line for the cross-section as a whole. Compare with Fig. 5. Note mismatches of adjacent elements at locations away from basal line. The dashed, horizontal line is taken as the approximate top of the formation.

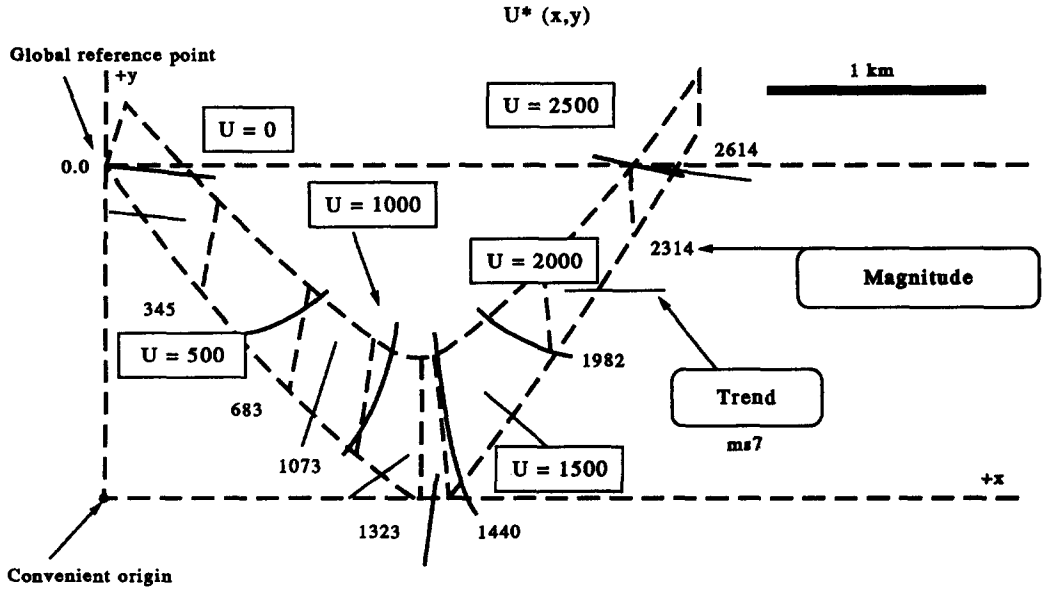

Fig. 7. The function $U^*(x, y)$ superimposed on an outline of the elemental version of the deformed cross-section (Fig. 4a). Note global reference point. Magnitudes of displacements along the base of the cross-section and the trends of iso-displacement lines at mid-points along the base of the elements were used to construct the function. The heaviest weight lines, labeled with values in multiples of 500 m, are iso-displacements lines for displacements in the x direction. The largest displacement called for by the restoration in the x direction is, for example, more than 2500 m.

that element. It must also, therefore, take into account displacement with respect to the global reference point as dictated by the fact that the point (1,3; adjusted) and (2,4) are the same. Thus, with $u^*(2,4)$ as the displacement in the x direction of point (2,4) with respect to the origin of second element, the origin of the second element must now be displaced an amount equal to $[-u^*(2,4) + 0 + u^*(1,3)]$ for the displacement to reflect the choice of the global reference point. The displacement in the x direction of point (2,3) with respect to the global reference point is $[-u^*(2,4) + u^*(2,3) + u^*(1,3)]$.

In this manner, displacement of all points in both the x and y directions are adjusted along the base of the cross-section. Results are shown in Figs. 7 and 8. Magnitudes of adjusted displacements are posted along the base of the cross-section.

The determination of iso-displacement lines for the function $U^*(x,y)$ is based on calculated values for $\delta U^*(x,y)/\delta x$ and $\delta U^*(x,y)/\delta y$ at the midpoint of the baseline for each element (equations 23–26). A local orientation for a contour of equal values of the displacements function can be obtained by noting that $\delta U^*(x,y)/\delta x$ is the rate of change in the function $U^*(x,y)$ in the x direction. It is the local 'apparent dip' of the function in the x direction. Similarly, $\delta U^*(x,y)/\delta y$ is the rate of change in the function $U^*(x,y)$ in the y direction, i.e. its 'apparent dip' in the y direction. From the 'apparent dips' of the function in two directions normal to each other (Ragan 1973, p. 4), one can compute the azimuth

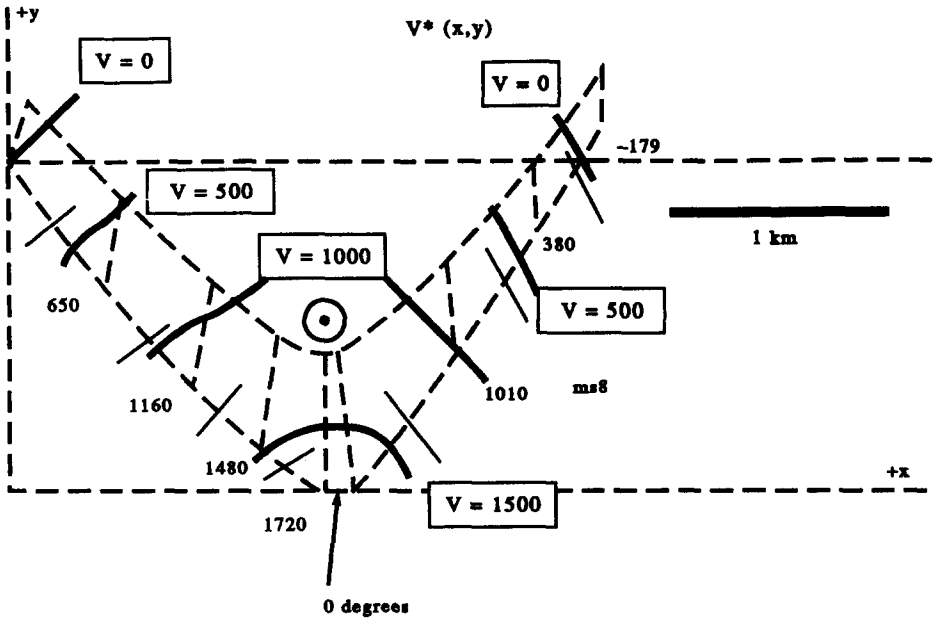

Fig. 8. The function $V^*(x, y)$ superimposed on an outline of the elemental version of the deformed cross-section.

and magnitude of maximum change in these functions (i.e. 'true dip'). Trend ('strike') lines lie at right angles to such azimuths. They provide the basis for drawing the iso-displacement lines.

Similar reasoning applies to the determination of the iso-displacement lines for the function $V^*(x,y)$. Figures 7 and 8 show trend lines posted where calculated, namely at the local origin for each element. They guide construction of iso-displacement lines as shown on these two figures.

Construction of the continuous displacements functions

We may now proceed to construction of continuous displacements functions. Construction is analogous to construction of a contour map. From information posted on magnitudes for displacements values and about trends of iso-displacement lines along the base of the elements, we may graphically construct lines of equal value of displacement for u^* and v^*. Figures 7 and 8 show iso-displacement lines. First-pass construction of these figures (i.e. Figs. 7 and 8) leads to a satisfactory restoration (Fig. 9, next section).

The usual problems of constructing a contour map from limited data likewise affect the graphical construction of displacement functions. A comprehensive discussion of possible techniques for construction of displacements functions, were it included in this article, would be similar to a discussion of the construction of a subsurface contour map from limited data. Different workers might well produce different 'maps'. However, information treated as control must be honored, and consequences of construction must pass certain tests. Our control included the displacements of selected points at the base of the elements and, also, the trend of the functions at the midpoints of the bases of the elements. Our construction, furthermore, passed an important test: it leads to a geologically reasonable restoration.

A particular complicating problem in constructing the displacements functions was minimized in our example, however. The problem is the assurance of continuity and compatibility for the displacements of points that make up the system of restored elements. Figure 6, for example, showed both gaps and overlaps, i.e. discontinuity and incompatibility. Continuity requires that there be no gaps between points of the system of elements. Compatibility requires that no two points move to the same location within the reference frame. We avoided this problem in our example by constructing continuous functions for the restoration of the system of elements based on control along the bases of the elements only and knowledge that the upper surfaces of the elements, when restored, had to be continuous and compatible. Both these conditions would be satisfied at the upper surface of the elements by a set of continuous displacements functions pertinent to that area. Problems of compatibility and continuity arise in restorations using complex systems of finite elements (e.g. Cobbold 1979) as discussed later in this paper. Because our procedure, for the particular example, led to a satisfactory result we did not pursue alternatives dealing with the upper surfaces of the elements. There are, however, opportunities for additional research on this topic.

USE OF DISPLACEMENTS FUNCTIONS TO EFFECT RESTORATIONS

Retro-deformation of the entire cross-section can now be done by applying the displacements functions shown in Figs. 7 and 8 to the deformed cross-section. Corner points of all the elements are retro-deformed as shown in Fig. 9. The base of the cross-section is restored to a continuous, horizontal state. The top of the restored cross-section is continuous but not quite flat, as shown by the dashed horizontal line. Perfect flatness could have been realized by slightly recontouring the displacements function $V^*(x,y)$ (Fig. 8). A shift downward of the 1000 m contour would result in a smaller displacement of the upper corners of element 5, in particular, and lead to a flatter upper surface. Likewise, some redrawing of the 0 (zero) contour could be done to bring the right-hand side of the upper surface of the resto-

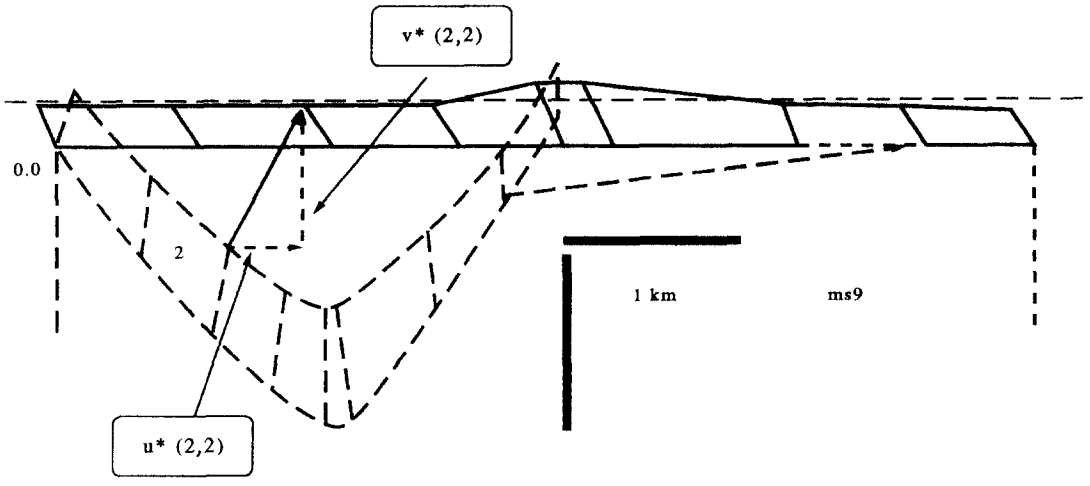

Fig. 9. Restoration of the cross-section based on continuous displacements functions shown in Figs. 7 and 8. Note the displacement of corner 2 of element 2, point (2,2) as well as point (7,3).

ration upward. First-pass constructions of U^* and V^* were done as a subsurface geologist would draw a contour surface with available control. However, it is reasonable, in view of available control, to adjust the contour map in order to yield a more acceptable geological result.

COMPARISON OF DISPLACEMENTS ANALYSIS WITH FINITIE ELEMENTS RESTORATION

Introductory remarks

Displacements analysis (Howard 1968a, and this paper) is concerned with discovering functions (e.g. Figs. 7, 8 and 9) that will return a deformed body to its undeformed state or to a prior state of deformation. Displacements analysis is, furthermore, related to another approach to restorations on which we will now comment: finite *elements* restorations (Oertel 1974, Oertel & Ernst 1978, Cobbold 1979, Woodward *et al.* 1986). As explained below, differences as well as similarities exist between these two approaches.

Differences and similarities in the approaches

The objective of the finite elements approach is the restoration of individual elements of a cross-section with good neighbor-to-neighbor contacts. Each element is restored by non-rotational unstraining and subsequent fitting of abutting boundaries (e.g. Fig. 6). Some applications of this method have included specific, post-unstraining rigid body rotations of elements (e.g. Oertel 1974, p. 450). Oertel & Ernst (1978, pp. 87–99) provide an example involving extensive element-by-element adjustments including rotations.

The critical technical problem for generating a solution using the finite elements approach is minimization of mismatches between individually restored, neighboring elements. Cobbold (1979) observed that up to the time of his publication "the fitting of elements. . . [had] been done piecemeal and by hand" and proposed a systematic procedure for improving on and measuring the goodness of fit of elements. So far as we are aware (see also Cobbold & Percevault 1983), however, the approach still leads only to restorations with minimal mismatches. Some mismatches are minor (Cobbold 1979, e.g. his fig. 5b), others significant (e.g. his fig. 6). Ideally, the procedures should lead to *no* mismatches because of requirements of continuity and compatibility in continuously deformed bodies. The displacements approach has no mismatches; they are removed as part of the technique for constructing the displacements functions. An exception occurs in situations involving faulting (Howard 1968c); then, discontinuities are designed into the functions.

Furthermore, the finite elements approach typically includes large, possibly unrealistic spatial gradients of strain at the boundaries of elements. The displacements approach leads to smooth, continuous functions and, therefore, smoothly and continuously varying strain. We believe that such variations are more likely to have developed naturally.

Although there are differences, there is an important, fundamental similarity between the two approaches. The restoration of individual finite elements involves displacements of points of elements. The construction of displacements functions is built, in large part, on information about the displacements of selected points of such restored finite elements, as explained above.

Additional features of the displacements approach

Two additional, attractive features of the displacements approach are as follows. First, improvements to a solution are fairly easy to make. This paper included an example involving consideration of changes to the first-pass displacements functions in order to make the upper surface of the cross-section perfectly flat. Second, the displacements vectors for the proposed functions provide insight into possible structural development through time. Envisioning the retro-deformation displacements functions as straight line vectors from the undeformed state to present deformation permits this insight. If we assume that the percentage-of-travel rate along such vectors is the same for all vectors, we may plot the change in shape of a surface through time. Percentage-of-travel is the fraction of total displacement realized at any time. The tips of the displacement vectors at a time of interest would position a surface of interest at that time. Figure 10, which is applicable to the procedures explained thus far, shows the upper surface of the cross-section at a time when half the total displacement of vectors from that surface has occurred. Using a selection of such surfaces (e.g. upper and lower surfaces of the cross-section) and a series of increments of time, one may construct an evolution of a deformed, continuous cross-section.

ONE-STEP VS MULTIPLE-STEP RETRO-DEFORMATION

Introduction

Our solution to this point has concerned comparison of two states of the material of the cross-section: present deformed state vs a completely undeformed state. We have not compared the present deformed state with one or more prior deformed states. In this sense, our solutions is 'one-step' and is typical of classical balancing restorations (e.g. Tearpock & Bischke 1991, pp. 403–419). The evolution of geologic structures often involves identifiable multiple stages of deformation (e.g. Protzman & Mitra 1990). In this section, we discuss restorations involving one identified intermediate stage of deformation. We recognize still more complex situations involving multiple stages of deformation, involving addition or removal of mass to a system, and/or involving faulting (i.e. discontinuous bodies; e.g. How-

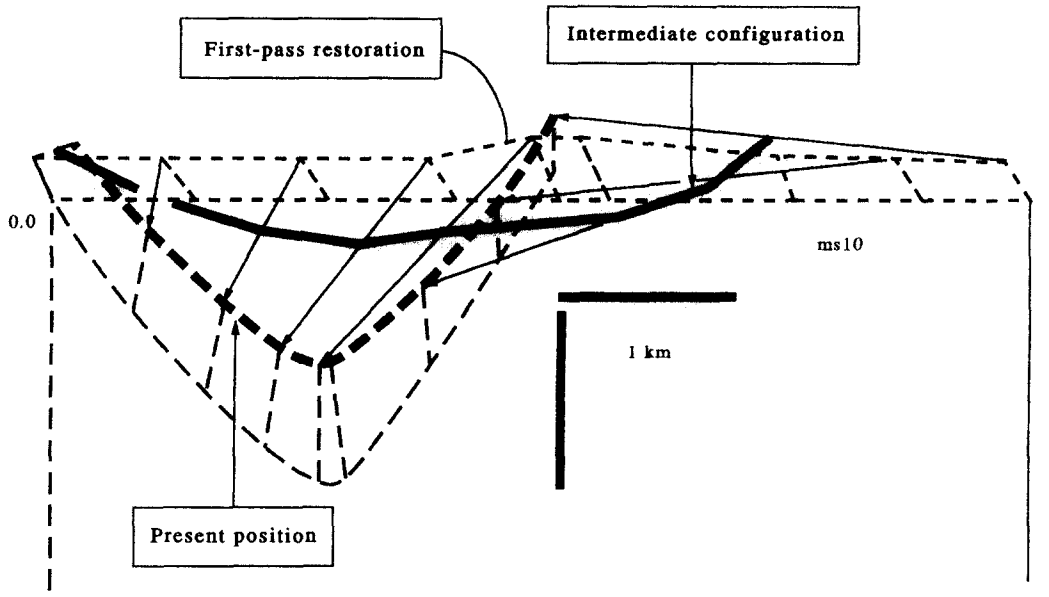

Fig. 10. Deformation of the cross-section from the first-pass restoration to the present deformation. The upper surface of the section in an intermediate stage configuration is shown by heavy line. Vectors are those required for the restoration but of opposite sign. Presumably half of the total movement on each vector has occurred at the same intermediate stage time.

ard 1968c). These are outside the scope of the present paper.

For situations involving an identified intermediate stage, the key idea is as follows. An intermediate stage is one to which a deformed state can be transformed; in turn, an intermediate stage can be transformed to an undeformed state. In this sense, the restoration is 'incremental'. The section from Woodward *et al.* (1986) once again serves as an example. The displacements approach can again be utilized and adapted to multi-step retro-deformation.

Discussion of example of Reks & Gray (1983) *and Woodward* et al. (1986)

Figure 9 implies that the strain ellipses posted on the deformed cross-section were the consequence of transforming flat-lying, unstrained strata to their present deformed condition. However, an alternative possibility exists, namely that reported values for strain are as a consequence of the transformation of an *a priori deformed state* to present deformation.

Reks & Gray (1982), the original authors of the section, drew the strain ellipses (Fig. 1) primarily from observations of chlorite fringes on pyrite crystals. They inferred that total fiber lengths record finite elongation in the rock (p. 171) and that the straight fibers of the fringes indicate coaxial deformation (p. 172). Reks & Gray (1983) further report that *as many pyrites as possible* were analyzed to check the similarity of strain estimates. These carefully gathered data, which are difficult to obtain and assess (e.g. Wickham 1973), provide an opportunity to demonstrate an alternative restoration as well as demonstrate the flexibility of the displacements approach to restorations. This alternative permits demonstration of a different *technique* to construct displacements fields. It demonstrates the inclusion of a specific, geologically hypothesized intermediate stage of deformation and emphasizes that certain strain indicators may record distinct increments of deformation (Howard 1968a, p. 1849).

The Woodward *et al.*–Reks & Gray rules for restoration to the configuration shown in Fig. 5 (bottom) were as follows: first remove strains from individual finite elements and second adjust the elements to match 'face centers of adjacent elements (Reks & Gray 1983, p. 119) (Fig. 6). Figure 15 from Reks & Gray (1983) indicates, furthermore, that the elements were all rotated so that the directions of greatest extension were vertical. This restoration (slightly modified, see below) is taken as a valid intermediate stage restoration through which a complete restoration must pass.

In principle, the technique for restoration used in the one-step solution could be applied. The orientations of bedding at the intermediate stage of deformation would not be flat but would be based on those of the intermediate stage fold (Fig. 5b.) There is, however, a direct approach. The Woodward *et al.*–Reks & Gray restoration permits graphical determination of displacements of selected points. Figure 11 shows the cross-section in present deformation superimposed on the Woodward *et al.*–Reks & Gray intermediate stage restoration. (We took the liberty of altering the third, fifth and seventh elements to make them compatible with their neighbors. Thus, Figs. 11 and 5 differ slightly.) The point (1,4) was again used as the global reference point. Selected, hand-measured vectors are shown on the figure. The vector displacements of all corners of the finite elements (not shown) were used to construct the displacement functions in Fig 12.

There are no recorded strains indicative of transformation from a flat bedded state to the intermediate state. Nevertheless, from an intermediate restored state, we may proceed to a completely undeformed state if we define the configuration of the latter. There are several reasonable choices, all with flat bedding. We chose to

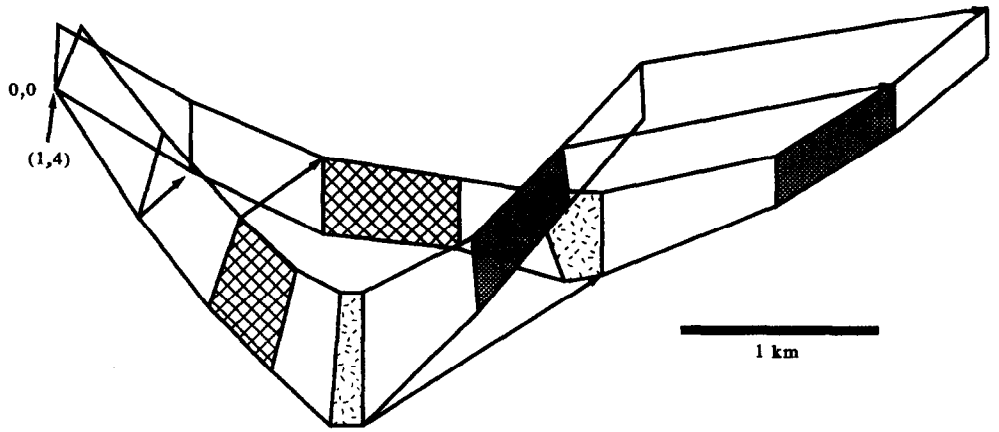

Fig. 11. Cross-section in present deformation superimposed on intermediate stage configuration based on an interpretation by Reks & Gray (1982, 1983). Displacements of selected points only are shown. Elements 3, 5 and 7 (patterned) are slightly modified from the original work (cf. fig. 5).

restore the intermediate stage to the form of a horizontal rectangle with area equal to the area of the intermediate stage cross-section. We put the lower left-hand corner of the rectangle at the global origin. We set its height equal to a thickness representative of the undeformed unit. The cumulative length of the upper surface of the intermediate stage section is about 2% shorter than its equivalent line in the undeformed state. The lower surface is slightly more than 3% longer. Accordingly, using graphical (cf. computational) methods, we transformed the bases and tops of each element to the undeformed state. Tops were shortened 2%; bases, elongated 3%. Figure 13 shows the results with selected vectors of displacement. Displacements for all corner points of elements were used to construct the displacements functions shown in Fig. 14.

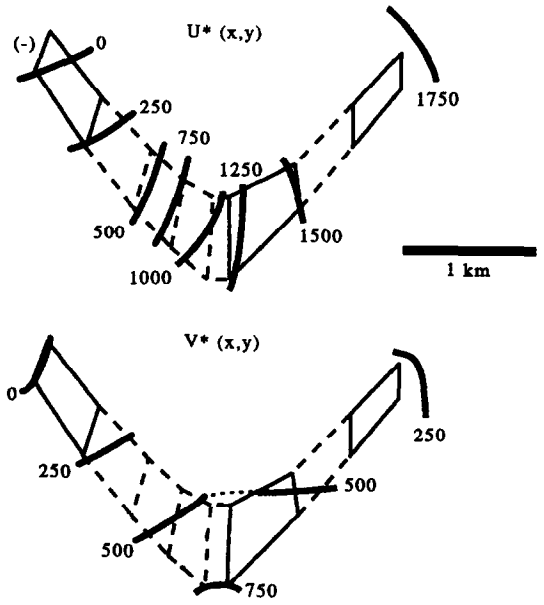

Fig. 12. Displacements functions for the retro-deformation of the present deformation to the configuration based on interpretation by Reks & Gray (1982). Note the required large displacements in the $+x$ direction at the right-hand side of the section. Note also the need for relative elevation of the central portion of the section.

Additional comments on one-step vs time-dependent retro-deformation

Comparison of the one-step solution and the solution incorporating an intermediate stage of deformation emphasizes a number of interesting points. First, the paths of displacements for the two solutions clearly differ. The combination of displacements shown in Figs. 12 and 14 do not yield the same paths for movement of points as does the one-step solution (Figs. 7 and 8). Hence, there are a number of ways to restore to an expected result, e.g. to flat bedding. Second, the implications of observed strain markers have to be carefully evaluated. A one-step solution may be appropriate. However, the chlorite fringes reported by Reks & Gray (1982, 1983) call for a multiple-step solution. The inclusion of information on various strain markers, including petrographic markers as noted by Wickham (1973) and Howard (1968a, pp. 1852–1853), should allow for more definitive restorations when such data are available.

SUMMARIZING REMARKS

We have explained a one-step procedure for restoring an unfaulted, variably strained cross-section. This procedure involves construction of retro-deformation displacements functions which summarizes the movements of points necessary to return—in one step—a strained, folded section to its undeformed configuration. The procedure has been successfully applied to a specific example section assuming that observed strain recorded transformation from an undeformed state to present deformation.

An alternative interpretation of observed strain is possible: observed strains indicate the transformation of the section from an intermediate deformed state to present deformation. The section may also be restored in a manner addressing this possibility, but this procedure requires multiple steps. The first step in the multiple step procedure was done by comparing the movement of selected points from the present deformed

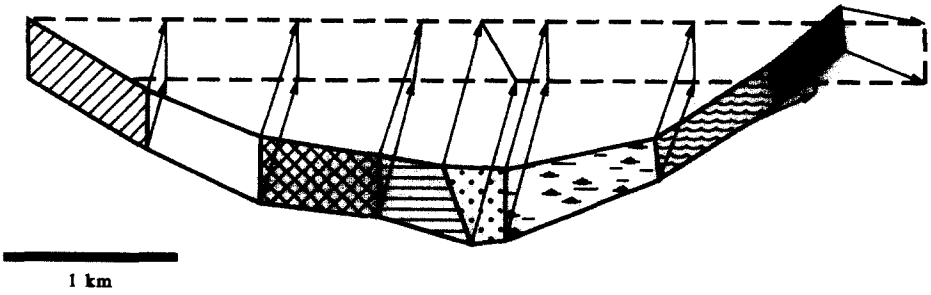

Fig. 13. Displacements of corner points of elements of the intermediate stage configuration to a completely undeformed state. The rectangle to which the fold is transformed has the same area as the folded section but has a uniform height equal to a thickness representative of the undeformed unit.

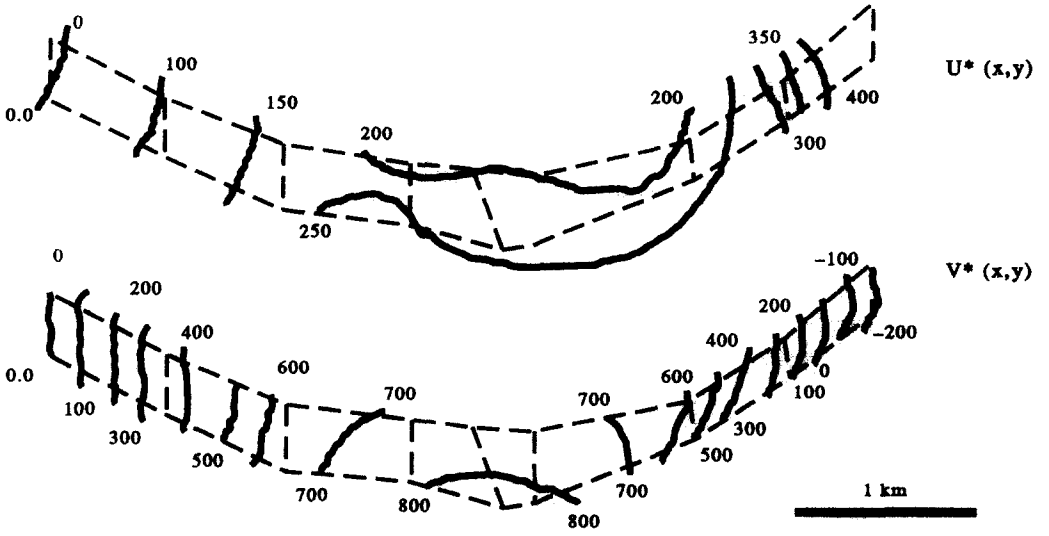

Fig. 14. Retro-deformation displacements functions for the transformation from the intermediate to undeformed states. Note upward movement with respect to the global reference point of the center of the folded layers but downward movement at its right-hand side.

state to an intermediate, more-open but folded state as originally proposed by Reks & Gray (1983). The second step involves the movement of selected points from the intermediate state to a particular undeformed configuration with area equal to that of the intermediate state. Each of these steps involves construction of sets of appropriate retro-deformation functions, which summarize movements needed to bring about full restoration through a specific intermediate state of deformation.

Acknowledgements—I wish to acknowledge reviews of two anonymous reviewers as well as *JSG* editor Professor Steven F. Wojtal. Each of these individuals patiently read the original draft of this paper and made specific suggestions for clarifying and enhancing it. I would also like to remember with gratitude the late John W. Handin, who was instrumental in providing me the initial opportunity to investigate problems of this type when we were both employed by Shell Development Company.

REFERENCES

Cobbold, P. R. 1979. Removal of finite deformation using strain trajectories. *J. Struct. Geol.* **1**, 67–72.

Cobbold, P. R. & Percevault, M.-N. 1983. Spatial integration of strains using finite elements. *J. Struct. Geol.* **5**, 299–305.

Jaeger, J. C. 1956. *Elasticity, Fracture, and Flow*. Methuen & Co., London.

Hodgman, C. D. 1959. *C.R.C. Standard Mathematical Tables* (12th edn). Chemical Rubber Publishing, Cleveland, Ohio.

Howard, J. H. 1968a. The role of displacements in analytical structural geology. *Bull. geol. Soc. Am.* **79**, 1846–1852.

Howard, J. H. 1968b. The use of transformation constants in finite homogeneous strain analysis. *Am J. Sci.* **266**, 497–506.

Howard, J. H. 1968c. Recent deformation at Buena Vista Hills, California. *Am. J. Sci.* **266**, 737–757.

Oertel, G. 1974. Unfolding of an antiform by the reversal of observed strains. *Bull. geol. Soc. Am.* **85**, 445–450.

Oertel, G. & Ernst, W. G. 1978. Strain and rotation in a multilayered fold. *Tectonophysics* **48**, 77–106.

Protzman, G. M. & Mitra, G. 1990. Strain fabric associated with the Meade thrust sheet: implications for cross-section balancing. *J. Struct. Geol.* **12**, 403–417.

Ragan, D. M. 1973. *Structural Geology—An Introduction to Geometrical Techniques* (2nd edn). John Wiley & Sons, New York.

Reks, I. J. & Gray, D. R. 1982. Pencil structure and strain in weakly deformed mudstone and siltstone. *J. Struct. Geol.* **4**, 161–176.

Reks, I. J. & Gray, D. R. 1983. Strain patterns and shortening in a folded thrust sheet: an example from the southern Appalachian. *Tectonophysics* **493**, 93–128.

Tearpock, D. J. & Bischke, R. E. 1991. *Applied Subsurface Geological Mapping*. Prentice-Hall, Englewood Cliffs, New Jersey.

Wickham, J. S. 1973. An estimate of strain increments in a naturally deformed carbonate rock. *Am. J. Sci.* **273**, 23–47.

Woodward, N. B., Gray, D. R. & Spears, D. B. 1986. Including strain data in balanced cross-sections. *J. Struct. Geol.* **8**, 313–324.